2D/3D seismic wavefield reconstruction for AVA imaging

Bin Liu and Mauricio D Sacchi, Department of Physics, University of Alberta, Henning Kuehl, Shell Canada*

Summary

In 2D/3D surveys, seismic data are often sparsely and irregular sampled along spatial coordinates. This introduces problems for multi-channel data processing techniques such as migration that often require a regular and dense spatial sampling. Wavefield interpolation can be used to produce densely and regularly sampled data, and therefore it is an effective mean to attenuate artifacts stemming from incomplete data acquisition.

The interpolation/re-sampling problem is posed as an inversion problem where from inadequate and incomplete data we attempt to recover the data we would have acquired with a denser distribution of sources and receivers. A minimum weighted norm interpolation (MWNI) method is used to interpolate prestack seismic data. In addition, we investigate the effectiveness of the 2D/3D MWNI scheme at the time of preconditioning seismic data for wave equation AVA imaging where a regular and dense data sampling is required to accurately estimate angle gathers.

Introduction

Seismic data are often sparsely and irregularly sampled along spatial coordinates. This produces problems for multi-channel processing techniques such as suppression of coherent noise (multiples and ground roll) and migration. Pre-stack interpolation of seismic traces is an effective mean to solve such problems. The interpolation/resampling problem can be posed as an inversion problem where from inadequate and incomplete data one attempts to recover a properly sampled version of the original seismic wavefield. The problem, however, is often effectively under-determined and, as it is well known, the solution is not unique. In this case, regularization methods can be used to estimate a unique and stable solution. Regularization serves to impose a particular feature on the solution (Cary, 1997; Sacchi and Ulrych, 1998; Duijndam et al., 1999; Hindriks and Duijndam, 2000; Liu and Sacchi, 2002). For example, minimum norm spectral regularization can be used when we assume that seismic data are band-limited in the spatial wavenumber domain (Duijndam et al., 1999; Hindriks and Duijndam, 2000). Similarly, a regularization derived using the Cauchy criterion can be used to obtain a high resolution (sparse) discrete Fourier transform that can be used to perform the synthesis of the data at new spatial positions (Sacchi and Ulrych, 1998). In the method of minimum weighted norm interpolation (Liu and Sacchi, 2002), we have used a spectral weighted norm regularization term that incorporates a priori knowledge of the energy distribution of the signal to interpolate. The technique can be used to simultaneously interpolate large portions of data along any number of spatial dimensions. It is important to stress that the MWNI algorithm is quite efficient; the computational cost of the interpolation relies on FFTs in conjunction with a pre-conditioned Conjugate Gradients scheme to accelerate convergence.

In this abstract, we present examples that illustrate the application of the MWNI algorithm to 2D/3D prestack seismic data. We also test the effectiveness of our interpolation strategy at the time of reconstructing data for 2D/3D wave equation AVA imaging.

Minimum weighted norm regularization

The one-dimensional MWNI algorithm (Liu and Sacchi, 2002) can be extended to higher dimensional algorithms using the properties of the Kronecker product of matrices (Davis, 1979). We denote N-dimensional (ND) sampling problem as $y = Tx$, where T is the sampling matrix of the problem, y and x are the vectors in lexicographic ordering of the elements of ND observations and unknowns, respectively. The ND MWNI solution can be obtained by minimizing following objective function

$$J(x) = \| Tx - y \|_2^2 + m^2 x^T Q x$$

where $\|\cdot\|$ stands l_2 norm, m^2 is a specified weighting factor that controls the trade off between the data norm and misfit of observations, and $x^T Q x$ defines the wavenumber domain weighted norm. In specifics, $Q = F_{ND}^T \Lambda F_{ND}$, F_{ND} is a ND Fourier transform matrix and Λ is a diagonal matrix with entries

$$\Lambda_{kk} = \begin{cases} 1/P_k^2 & k \in \Omega_{ND} \\ 0 & k \notin \Omega_{ND} \end{cases}$$

where Ω_{ND} denotes indexes for the pass-band of the data and P_k^2 is a positive function which is similar in shape to the power spectrum of the ND unknown data in lexicographic form. The key to a successful reconstruction is to define a DFT-weighted norm that resembles the spectrum of the true solution. In particular, since the interpolation is always performed at one temporal frequencies at the time (fx type interpolation); we found that the weights used to interpolate the spatial signal at

temporal frequency f can be derived from already interpolated data at frequencies f_1, f_2, f_3, … A similar strategy is described in Hugonnet et. al (2001) to estimate weights in the high resolution Radon transform.

Example: Marmousi Dataset

The performance of the 2D MWNI algorithm is first demonstrated with the Marmousi dataset. The original Marmousi shot and receiver sampling intervals are both 25 meters. We simulate a new survey with 75 meters shot - receiver intervals. The seismic traces from the new survey are input to our interpolation algorithm. We first perform Fourier transform along the time axis. Reconstructions are then carried out at temporal frequencies along two spatial (shot and receiver) coordinates simultaneously. All the missing traces have been reconstructed. The details of the reconstruction at shot positions 3075m, 3100m and 3125m are shown in Figure 1a-1b. Figure 1a portrays the incomplete shots, Figure 1b shows the reconstructed shot records. Next, we migrate the complete, incomplete and reconstructed datasets with a wave equation DSR AVA migration algorithm (Prucha et. al, 1999). Figures 2a, 2b and 2c show both the stacked image and the migrated CIG at CMP location 7500m using the three different datasets. The migration with the complete dataset yields the stacked and CIG images portrayed in Figure 2a. The coarse sampling of the decimated wavefield results in severely aliased events in both the stacked image and the CIG (Figure 2b). In Figure 2c, we observe that the migration with the reconstructed wavefield yields an overall better stacked image without visible signs of aliasing. The continuity of events in the CIG is also improved. To study the impact of wavefield interpolation on AVA analysis, a depth point located in the upper half of the model is chosen for AVA inversion. Note that the picked target phase in the CIG is indicated with an arrow in Figure 2. In Figure 3a, the reflection coefficient based on the acoustic approximation shows an increasing trend with the angle of incidence on the theoretical AVA curve. Despite its roughness, the AVA curve picked on the migrated CIGs obtained with the complete data agrees with the theoretical AVA trend. The AVA curve picked on the migrated CIG from the reconstructed wavefield (Figure 3b) is much closer to the original one when compared to the one picked on the migrated CIG in Figure 3a.

Example: 3D Common Azimuth Dataset

We have applied the MWNI pre-stack interpolation to a 3D real seismic dataset. The complete dataset contains 150 inlines and 40 crosslines with offsets aligned along the inline direction. The offset distribution in each CMP bin is illustrated in Figure 4a. Pre-stack interpolation is simultaneously applied along three dimensions, namely: inline-midpoint, crossline-midpoint and offset. Figure 4b shows the original CMPs for inline #6 and crosslines #15-18. The reconstructed result is shown in Figure 3c. Notice that all the gaps have been filled.

3-D common azimuth wave equation DSR AVA migration is applied to both the original and the interpolated datasets. Figures 5a and 5b show the migrated image for crossline #36 and inline #71; in both cases data before interpolation was used in the migration. Note that the irregular and sparse data sampling results in images of poor quality. Migrated images obtained with the interpolated data are portrayed in Figures 5d and 5e. The improvement on the stacked image can also be seen from depth slices. In Figure 5c and 5f, we show depth slices (depth=1470m) extracted from the migrated cube obtained with the raw and the interpolated data, respectively. The impact of interpolation before AVA imaging can also be seen in the ray parameter CIG domain. CIG gathers for crossline#36 and inline#71 are shown in Figures 5g and 5h. The migration with the interpolated data as input yields a CIG gather (Figure 5h) with reduced artifacts and better event continuity.

Conclusions

In this abstract, we applied the MWNI reconstruction algorithm to pre-stack seismic before wave equation AVA migration. The method enables us to incorporate both the band-width and the signal spectrum shape into the interpolation problem and, therefore, it often yields optimal reconstructions. The method is extremely efficient since all computations are done in the flight using FFTs and a preconditioned conjugate gradients algorithm. It is important to mention that the method can be applied to seismic data in any domain with multiple spatial coordinates. Finally, examples with synthetic and real 3D data show an important reduction of sampling artifacts both in the stacked image and in individual AVA gathers.

References

Cary, P., 1997, High-resolution "beyond Nyquist" stacking of irregularly sampled and spare 3D seismic data: Annual Meeting Abstracts, CSEG, 66-70.

Davis, P. J., 1979, Circulant matrices. New York: Wiley.

Duijndam, A.J.W., Schonewille, M., and Hindriks, K., 1999, Reconstruction of seismic signals, irregularly sampled along on spatial coordinate: Geophysics, 64, 524-538.

Hindriks, K. O. H., Duijndam, A.J.W., 2000, Reconstruction of 3-D seismic signals irregularly sampled along two spatial coordinates: Geophysics, 65, 253-256.

Hugonnet, P., Herrmann, P. and Ribeiro, C., 2001, High Resolution Radon - a Review, 63rd Mtg.: Eur. Assn. of Expl. Geophys., Session: IM-2.

Kuehl, H., 2002, Least-squares wave-equation migration/inversion: Ph.D. thesis, University of Alberta.

Liu, B., and Sacchi, M.D., 2002, Minimum DFT-weighted norm interpolation of seismic data using FFT: Annual Meeting Abstract, CSEG.

Prucha, M., Biondi, B., and Symes, W., 1999, Angle domain common image gathers by wave-equation migration, 69th Ann. Internat. Mtg., Soc. Expl. Geophys., Expanded Abstracts, 824-827.

Sacchi, M.D., Ulrych, T.J., and Walker, C., 1998, Interpolation and extrapolation using a high-resolution discrete Fourier transform: IEEE Trans. Signal Processing, vol. 46, no. 1, 31-38.

Acknowledgements

The Signal Analysis and Imaging Group at the University of Alberta would like acknowledge financial support from the following companies: Encana, Geo-X Ltd., and Veritas Geoservices. This research has been also partially supported by the Natural Sciences and Engineering Research Council of Canada, the Alberta Department of Energy and by the Schlumberger Foundation. Field data has been generously provided by Veritas Geoservices.

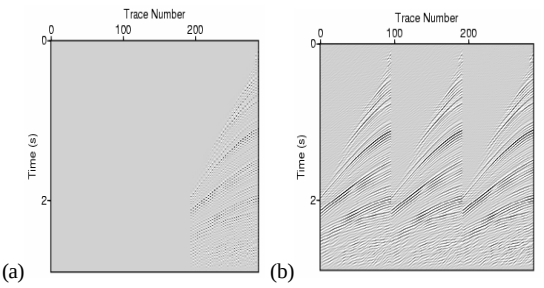

Figure 1: (a) Decimated shot gathers at 3075m, 3100m and 3125m. (b) Reconstructed shot gathers.

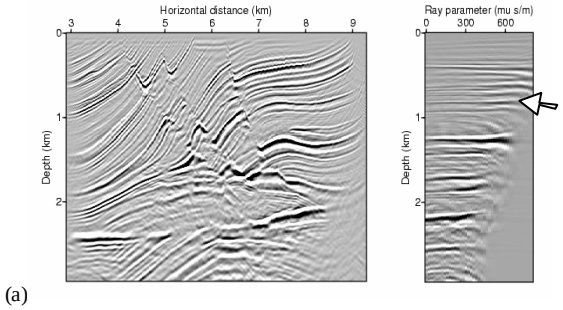

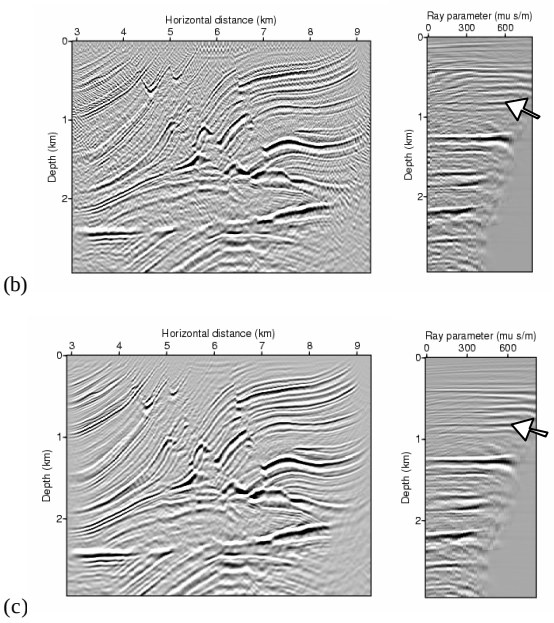

Figure 2: (a) Migrated image of the Marmousi model and CIG at CMP location 7500m. All the dat a were used in the migration. (b) Migration of the Marmousi model using the decimated data. (c) Migration of the Marmousi model using the reconstructed data.

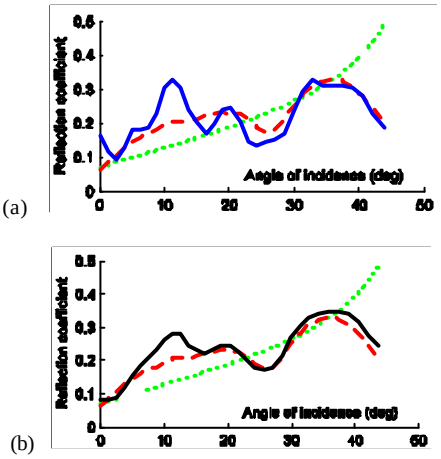

Figure 3: (a) Theoretical (Green) and extrated AVA curves from the migrated angle gather (Red: orginal complete data, Blue: decimated data). (b) Theoretical (Green) and extracted AVA curves from the migrated angle gather (Red: original complete data, Black: after interpolation).

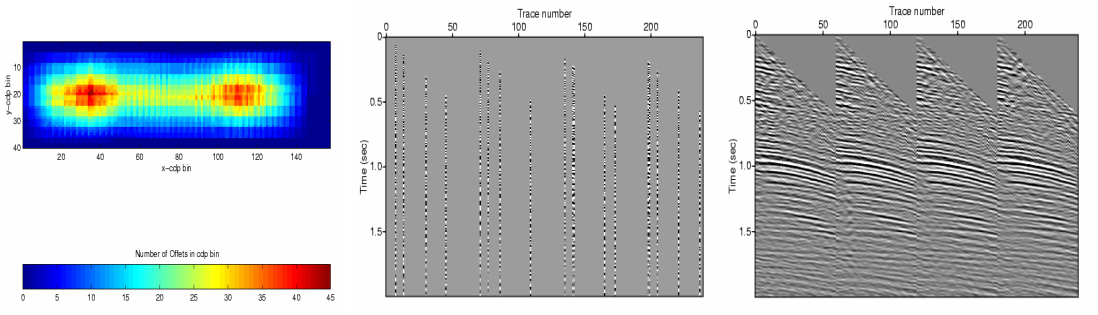

(a) (b) (c)

Figure 4: (a) Distribution of offsets for the 3D field data used to test our interpolation algorithm. (b) The original traces in four adjacent CMPs corresponding to inline # 6 and crossline #15-18. (c) The reconstructied data after 3D MWNI.

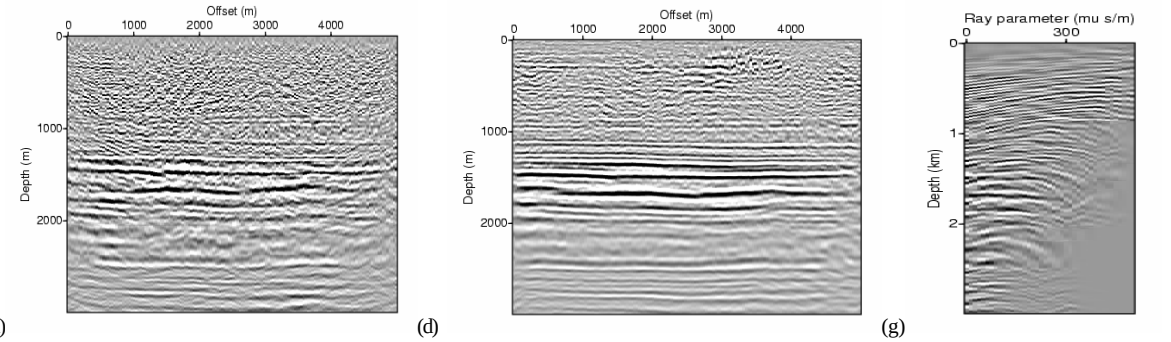

(a) (d) (g)

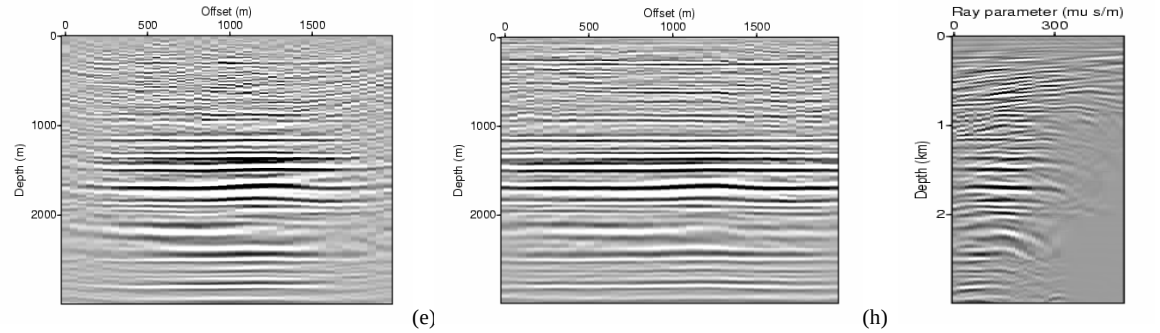

(b) (e) (h)

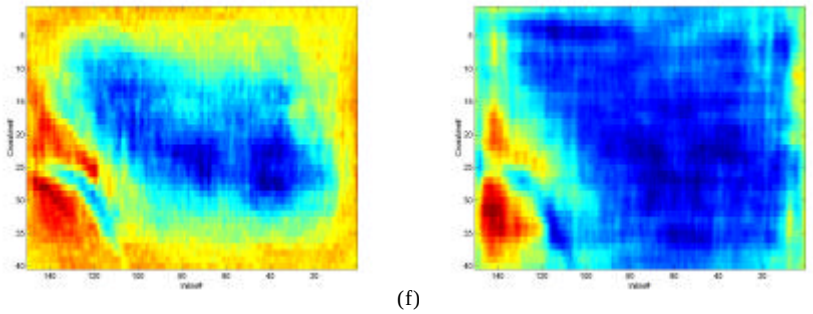

(c) (f)

Figure 5a,b and c: crossline, inline and depth slice of migrated 3D common azimuth data without interpoation. d,e, and f: images obtained by migrating the interpolated data. g and h: CIGs obained with the undersampled data (original pre-stack volume) and the reconstructed data, respectively.